LAL 87-48
Sept. 1987

Laboratoire de l'Accélérateur Linéaire

Hard Electromagnetic Processes

François RICHARD

Rapporteur's talk at the 1987 International Symposium on Lepton and Photon Interactions at High Energies Hamburg, July 27-31, 1987

U.E.R
de
l'Université Paris-Sud

Institut National
de Physique Nucleaire
et
de Physique des Particules

Bâtiment 200 - 91405 ORSAY Cedex

LAL 87-48
Sept. 1987

HARD ELECTROMAGNETIC PROCESSES

François RICHARD

Laboratoire de l'Accélérateur Linéaire, 91405 Orsay, France

INTRODUCTION

A review of the very many experiments dealing with "hard electromagnetic processes" goes far beyond this talk. I will, instead, use the most recent data and focus on quantitative test of QCD. More specifically, I will retain two items :

- hadroproduction of direct photons,
- Drell-Yan.

In addition, I will briefly discuss a recent analysis of ISR data obtained with AFS (Axial Field Spectrometer) which sheds a new light on the e/π puzzle at low P_T.

Readers interested can find extensive reviews on Drell-Yan and direct photons in ref. 1.

HADROPRODUCTION OF DIRECT PHOTONS

Recent data

Let me first describe the data collected recently and recall the basic experimental limitations.

1. Fixed target

Fixed target experiments at SPS have accumulated large luminosities with highly segmented calorimetry (Table I). They obtain clear prompt γ signals with good rejection against π^0,η backgrounds dominant at low P_T. They also can efficiently reject the muon halo background, mostly relevant at large P_T, using timing and angular measurement.

In spite of the high quality of these data, the systematical errors are still of order 20 to 30 %. They are due to well known limitations which I briefly recall :

- the background substraction which gives a source of 10 to 20 %. A detailed simulation is used to reproduce experimental distributions. However, given the

numerous effects involved (materialization of photons, coalescence for energetic π^o, η contribution, etc...) experimentalist take a conservative attitude in their estimates,

- the energy scale can be precisely calibrated to within 1 % using the π^o and η mass distributions. With the very steep slope in P_T of the photon distribution, a 1 % uncertainty corresponds to about 10 % error on the cross section,
- an additional 10 % uncertainty is added to take into account luminosity monitoring and various inefficiences.

TABLE I. Fixed target (hydrogen) experiments

Experiment	Beam	Sensitivity pb^{-1}	Lab energy GeV	Photon detection	Hadron detection
NA24	π^- π^+ p	1.3 0.2 0.45	300	Prop. tubes 9X° Pb/scint. 16X°	Segmented had. cal.
WA70	π^- π^+ p	3.5 1.3 5.2	280	Pb/liquid scint. 24X° in 3 segments	Ω spectrometer
UA6	$\bar{p}$	0.5	315	Pb/prop. tubes 24X° in 3 segments	Magnet spectrometer

When considering the X_F distributions, say at fixed P_T, one should also realize that they usually correspond to a vast dynamical range in the photon energy. Additional systematical errors can then occur which are due to linearity problems or to rapid changes in background contributions. In comparing data and predictions, I will therefore privilege P_T distributions which are less affected by these uncertainties.

2. Colliders

Since the first results coming from ISR, it has been realized that the prompt photon signal is cleaner at high energies for a given X_T. As will be shown shortly, these data complement very well the kinematical domain covered by the fixed target results.

Up to now, no fine grain calorimetry with large solid angle coverage could be designed : at ISR, R806[2] was using highly segmented liquid argon calorimeter with Ω = .2str while R110[3], UA1[4] and UA2[5], which use a cruder calorimetry, request an isolated electromagntic cluster with additional criteria based on distinct shower patterns for photons and π^o (table II).

TABLE II. Collider experiments

Experiment	Sensitivity pb^{-1}	Photon detector	Method
ISR	($\sqrt{s}$ = 63 GeV)		
AFS	17	NaI(6X°)+ U calorimeter	Direct + isolation
R110	250	Pb Glass + MWPC	Cluster shape + isolation
R806	50	Pb/liq. Argon finely segmented	Direct
$S\bar{p}pS$	($\sqrt{s}$ = 630 GeV)		
UA1	0.57	Pb/scint. 4 samplings + had. cal.	Longitudinal sampling + isolation
UA2	0.31	Preshower 1.4 X° Pb/scint. + had. cal.	Conversion probability + isolation

As an example, let me sketch the method used in UA1 to extract the prompt photon signal. Firstly they can make full use of the isolation criteria with both charged and neutral particles. Second they use the longitudinal sampling of the electromagnetic shower to discriminate between direct photons and jets

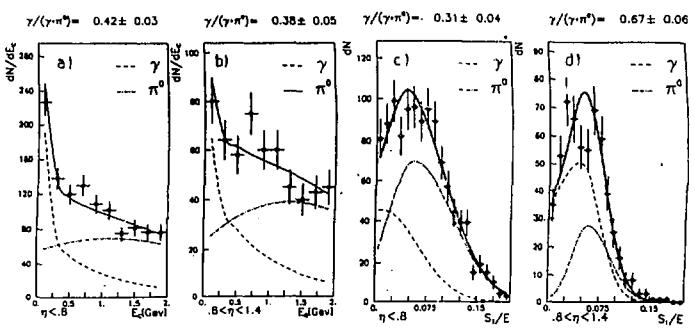

FIGURE 1

Figure (a) and (b) display the energy distribution around the cluster observed for photon candidates in the two rapidity regions. Curves are expectations for π^0 (ISAJET) and photons (minimum bias). Figure (c) and (d) show the distribution of the energy fraction deposited in the first sampling of the UA1 calorimeter with the corresponding expectations for π^0 and γ.

consisting of one or several π^0 or η. The background is simulated using ISAJET while the signal is generated assuming isolated photons plus particles coming from the so called minimum bias contribution. Plots shown in figure 1 illustrate the various distributions obtained and the quality of the separation.

This type of procedure carries obviously more uncertainties than the classical method used for fixed target. UA1 estimates, in addition, an error of 3 % on the absolute energy and a 15 % uncertainty on the luminosity.

Theory

Before comparing data and predictions based on perturbative QCD, it seems necessary to summarize the problems encountered so far and to discuss, in a somewhat simplistic way, some recent theoretical developments triggered by these problems.

1. Basic processes

At lowest order, hadroproduction of prompt photons is explained by two processes involving a gluon (Fig. 2). The annihilation diagram is dominant for

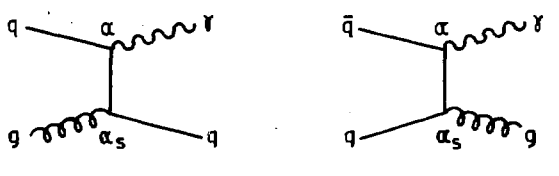

FIGURE 2
Basic processes, at $O(\alpha_s)$, contributing to hadroproduction of direct photons

$\bar{p}p$ and $\pi^- p$ processes at large X_T where a valence antiquark $\bar{u}$ from the projectile annihilates with a valence quark u from the target. In $\pi^{\pm} p$, where the valence antiquark $\bar{d}$ from the projectile has a small electromagnetic coupling and in pp, where no valence antiquark is available, the Compton diagram dominates. This is also the case in $p\bar{p}$ for collider data at low X_T.

At order α_s^2, very complex calculations were performed[6]. Contogouris et al.[7] give an approximate formula based on the dominance of the soft gluon contribution. Each of the two basic processes gets multiplied by a "K factor",

terminology inherited from Drell-Yan, of the form :

$$K = 1 + \frac{\alpha_s(Q^2)}{2\pi} C \pi^2$$

where $K_{Compton} \sim 1.8$ and $K_{annihilation} \sim 1.5$.

2. What is Q^2 ?

The large Q^2 appearing in QCD perturbative calculations is not unambiguously related to the kinematics of the reaction. In a very comprehensive review of the data recently given by J.F. Owens[8], it is found that with $Q^2 \sim c\ P_T^2$, where c varies typically between 1/2 and 4 depending on the reaction, one can reproduce reasonably well the data with the perturbative QCD calculations at leading order. To lllustrate the impact of this uncertainty, let me take the reaction $p\bar{p} \rightarrow \gamma X$ at $x = 0.4$, where the annihilation term dominates. With the two extreme possibilities previously defined, α_s varies by - 40 % while the structure function $F_2(x)$, which appears quadratically in this process, varies by - 25 %. From this example, one simply understands why such ambiguities introduce an uncertainty of a factor 2 or more in these calculations. As rightly commented in ref. 8, this ambiguity is more important than the approximate K factor effect previously mentioned !

Exact order α_s^2 calculations improve the situation, as discussed in ref. 9 contributed to this conference. When we change the definition of Q^2 the variation in the Born term is compensated to order α_s^2 by a variation in the H.O. term, such that :

$$\sigma^{(2)}\ (Q'^2) = \sigma^{(2)}\ (Q^2) + O(\alpha_s^3)$$

This cancellation brings down the uncertainty to about 50 %.

A further improvement is still necessary to cope with the present experimental accuracy.

Two criteria have been proposed. Stevenson[10] and Politzer[11] remark that the Q^2 dependence disappears when the cross section is computed at all orders so that $d\sigma/dQ^2 = 0$. They propose to use this criterion to define, at a given order, the effective value of Q^2 : Q^2_{opt}. Grunberg[12] has proposed to use a definition of Q^2 which cancels the higher order (H.O.) correction to insure a fast convergence of perturbative calculation.

In ref. 9, these two methods are applied using the full H.O. calculation and give similar results. $\alpha_s\ (Q_{opt})$ is small in the relevant physical region ($P_T > 3$ GeV, for fixed target) implying that this approach is meaningful and that the convergence is fast. It is thus reasonable to expect small $O(\alpha_s^3)$ contributions, presumably below 20 %. Other sources of uncertainty, that I will discuss in the next §, could, in this new context, become more important.

3. Remaining uncertainties

3.1 Intrinsic K_T smearing

We know[8], from Drell-Yan processes, that the intrinsic transverse momentum given to the partons is of order 500 MeV when H.O. terms, like real gluon emission, are included. One can thus expect modest corrections due to this effect. Unfortunately there is no standard way to perform this calculation which is quite model dependent[8].

3.2 Higher twist

E.L. Berger[13] has shown how higher twist effects can be estimated (figure 3)

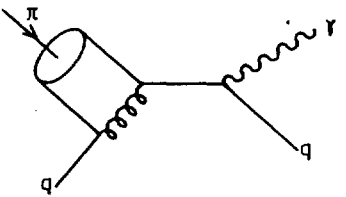

FIGURE 3
Example of higher twist process contributing to pi-production of direct photons

in $\pi p \to \gamma X$ processes. He concludes that, except at large X_F where they might become noticeable, higher twist corrections are at the per cent level.

3.3 Bremsstrahlung

Quarks can radiate photons in the various parton sub-processes (e.g. figure 4). These processes are of order α_s^2; since the photon fragmentation function is proportional to α/α_s, the resulting contribution is of order $\alpha\alpha_s$ comparable to the Compton and annihilation processes. From theory[9,14] and

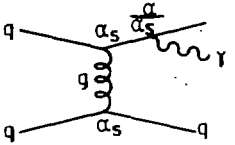

FIGURE 4
Example of quark bremsstrahlung effect in a parton sub-process

from experiment[15], one estimates a 20 % contribution from this mechanism at ISR. Larger effects are estimated at the $Sp\bar{p}S$ collider but they are strongly reduced by the isolation cut used in the analysis. These small corrections have been included in the optimisation procedure and one concludes that this effect is well under control.

3.4 Structure functions.

We will be using structure functions determined by Duke and Owens from DIS, Drell-Yan and Υ hadroproduction[16,17]. As well known, the DIS and Drell-Yan data provide poor knowledge about the gluon structure function . In particular, one finds a strong correlation between Λ and the gluon distribution function. This has led Duke and Owens to propose two sets of solutions compatible with the available data. DOI structure functions correspond to a soft gluon structure function and $\Lambda_{\overline{MS}}$ = 200 MeV, while DOII has $\Lambda_{\overline{MS}}$ = 400 MeV and a hard gluon function.

It is clear that the situation is now evolving with the advent of more precise data[18]. New sets of distribution functions should be tried in the near future.

Let me finally remark that I will not include in my presentation data on nuclei, thus avoiding any reference to the EMC type effect.

4. Conclusion on theory

From the previous discussion, one may conclude that the main uncertainties in QCD calculations come from $\Lambda_{\overline{MS}}$ and the gluon structure function.

Nowhere else did we find a major uncertainty which prevents us from hoping that these calculations are at a 20 % level. Only through a detailed comparison between theory and experiment can we reach a final verdict.

Experiment versus theory

I will first discuss reactions dominated by the annihilation process for which the structure functions are well measured. They will give a direct determination of α_s, or equivalently $\Lambda_{\overline{MS}}$. Given the preliminary status of some of these data, I will discuss the determination at a semi-quantitative level, indicating the general trend. Unless explicitly stated, the theoretical predictions come from ref. 9.

1. Annihilation dominated reactions

1.1 For $p\bar{p} \to \gamma X$, in the X_T domain covered by UA6[19], the annihilation term represents about 80 % of the cross section. Since the proton structure function

is simply related to DIS, this process is ideally suited for determining α_s. In figure 5, the two DO parametrizations with $\Lambda_{\overline{MS}}$ = 200 MeV and $\Lambda_{\overline{MS}}$ = 400 MeV are clearly discriminated by the data in favor of the former. In figure 6

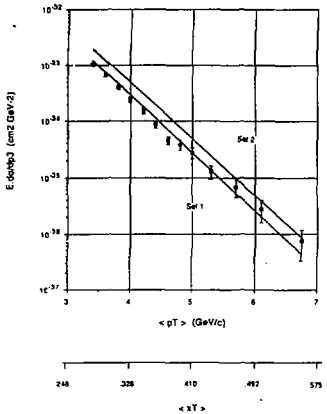

FIGURE 5
Preliminary results from UA6 on $\bar{p}p \rightarrow \gamma X$ at $\sqrt{s}$ = 24 GeV. Set 1 and 2 curves correspond to DOI and DOII referred in the text.

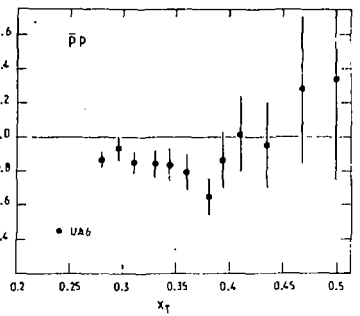

FIGURE 6
Same data as in figure 5 where one displays the ratio data/prediction, using DOI. Errors are statistical only.

I display the ratio data/prediction with $\Lambda_{\overline{MS}}$ = 200 MeV. If one changes $\Lambda_{\overline{MS}}$ to 100 MeV, this ratio moves up by 25 %, giving an improved agreement. Before drawing any definite conclusion, one should however remember that the systematical errors, not yet given in this preliminary data, are of the same order.

1.2 In $\pi^- p$, where the π gluon structure function is harder, about 60 % of the cross section comes from annihilation. The comparison is done including data from NA24[20] and WA70[21] on figure 7. The consistency between the two sets of data and the agreement with theory are impressive. $\Lambda_{\overline{MS}}$ = 200 MeV seems preferred to $\Lambda_{\overline{MS}}$ = 100 MeV.

With the high statistics available on $\pi^+ p \rightarrow \gamma X$ in WA70, one can directly access to the annihilation terms by plotting the difference $\pi^- - \pi^+ \rightarrow \gamma X$.

Figure 8 confirms, with rather large statistical errors, that $\Lambda_{\overline{MS}}$ = 200 MeV is the preferred value.

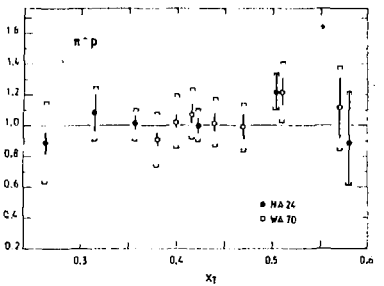

FIGURE 7
Results from NA24 and WA70 on $\pi^- p \to \gamma X$ where the ratio data/prediction is obtained using DOI. Experimental errors([ ]) are obtained by adding quadratically statistical and systematical errors.

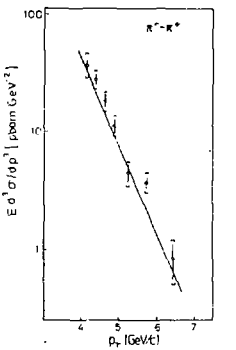

FIGURE 8
Results from WA70 on the difference $\pi^- - \pi^+ \to \gamma X$. The curve uses DOI.

2. Compton dominated reaction

Assuming that $\Lambda_{\overline{MS}}$ is fixed to 200 MeV, a value compatible both with $\bar{p}$ and π^- data, one can now use Compton dominated processes to extract information on the gluon structure function.

2.2 pp data

In figure 9, the WA70[22] pp data, at $\sqrt{s}$ = 23 GeV, are in good agreement with the prediction of Aurenche et al[9] using DOI structure functions. DOII structure functions are rejected for two reasons. Firstly, there a factor of about 3 in normalisation coming from α_s ($\sim \times 1.5$) and from G(x) ($\sim \times 2$) the gluon structure function. Second, one can observe a difference in slope which originates from the different dependence in x :

$xG_I(x) \sim (1-x)^6$

at $Q^2 = 4$ GeV^2

$xG_{II}(x) \sim (1-x)^4$

NA24 data confirm this conclusion.

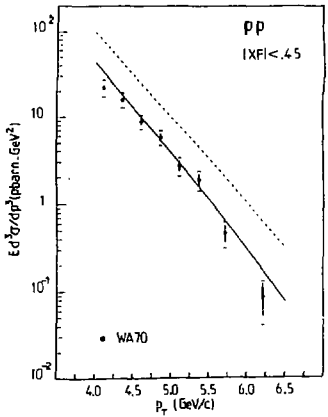

FIGURE 9
Results from WA70 on pp → γX selecting $|X_F| < 0.45$. The dashed curve corresponds to DOII, the full curve to DOI.

The collider data, which cover the low X_T region, are dominated by the Compton contribution. As mentioned previously, UA1[14] has measured the process pp → γX for isolated photons. In figure 10 the data are shown in the central region (pseudo rapidity < 0.8) and in the forward region (pseudo rapidity between 0.8 and 1.4). The dashed curves give the total rate of direct γ while the full curves correspond to a theoretical estimate[23] of the direct γ with isolation criterion. Both sets of curves differ at low P_T where the effect of bremsstrahlung is quite substantial. In figure 11, data from UA1 are compared to data from UA2, showing good agreement.

These data are not very sensitive to the choice of the gluon structure function. At large Q^2, as discussed in ref. 8 , both sets turn out to be quite similar since scale breaking effects will act differently on the soft and hard gluon distributions.

At ISR, the direct photon signal is extracted using either the standard method (R806) or some shower pattern methods plus isolation criteria. The agreement, as shown is figure 12, is reasonable, but certainly not at the level

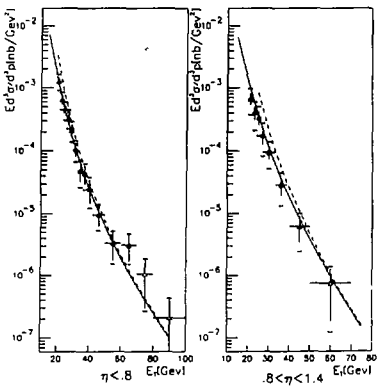

FIGURE 10
Preliminary results from UA1 on $p\bar{p} \rightarrow \gamma X$ for two rapidity domains. The dashed curve corresponds to the total γ yield, while the full curve is for γ isolated within a cone of 57° aperture.

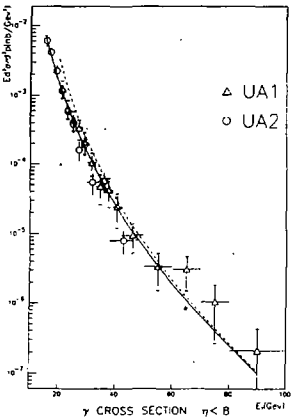

FIGURE 11
Comparison between UA1 and UA2 data in the central rapidity region. Curves are defined as in figure 10.

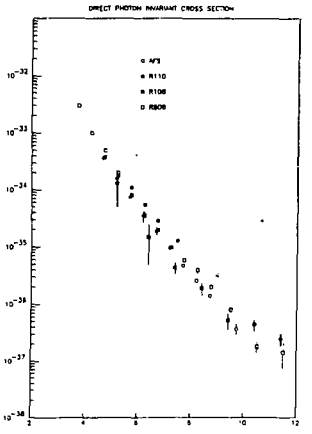

FIGURE 12
Comparison between the ISR data for $pp \rightarrow \gamma X$. The data from R110 are preliminary. Errors are statistical only.

one would need for an accurate test of QCD. In their preliminary version, the recently analysed data from R110, with very high statistics, are well above the old R108 data but also do not agree too well with the R806 data. For the time being, I will use the latter for comparison with QCD.

Figure 13 shows the overall comparison using DOI. Given the systematical errors, one can be content with no further adjustments. It is however tempting

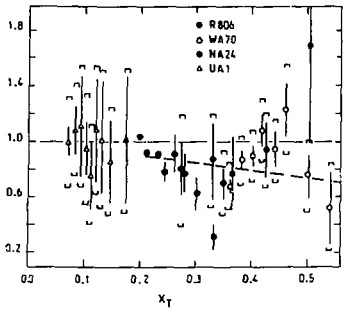

FIGURE 13
Results from pp → γX from fixed target and ISR (R806) where the ratio data/prediction is obtained using DOI. UA1 data, at low X_T, are also included. The dashed line corresponds to an increase of 0.5 in the power law of $xG(x) \sim (1-x)^{\eta}$.

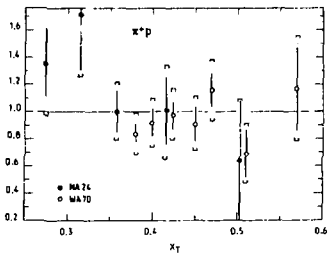

FIGURE 14
Results from NA24 and WA70 on $\pi^+ p \to \gamma X$ where the ratio data/prediction is obtained using DOI.

to move slightly the x dependence in $G_I(x)$ to improve the agreement with theory at large X_T. With $\Delta\eta_G = +0.5$ in $xG(x) \sim (1-x)^{\eta_G}$, one finds indeed a better adjustement. The corresponding displacement at large X_T shows the high degree of sensitivity of this reaction to small changes in η_G. One can for instance easily exclude the much steeper dependence suggested by a recent analysis of DIS data[18]. One should however stress that the DIS analysis only concerns the low x region, while our conclusion mainly concerns the region above x = 0.3.

2.2 π^+ p data

The data from NA24 and WA70 at $\sqrt{s}$ = 23 GeV are well adjusted by the DOI set (figure 14). To eliminate, at first order, the effect of α_s, one usually plots the ratio π^-/π^+. This is shown in figure 15 for both experiments.

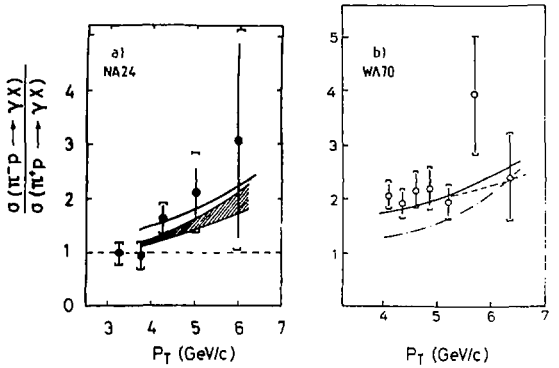

FIGURE 15
Measured π^-/π^+ ratio for NA24(a) and WA70(b). Full curves are predictions using DOI. Dashed curve in b is for DOII. Predictions from Contogouris et al.[24] are shown on a with their uncertainty (hatched area) and on b (dashed dotted curve)

The full curve, corresponding to Owens I choice, is in good agreement with the data. Owens II set gives very similar results as shown in figure 15b. This result is readily understood if one recalls that[17] :

$$xG_I(x) = 0.9\,(1-x)^{3.11}\,(1+6x)$$
$$xG_{II}(x) = 0.8\,(1-x)^{2.89}\,(1+6x) \qquad \text{at } Q^2 = 4 \text{ GeV}^2$$

One may also notice that no spectacular rise of the ratio is observed between $P_T = 4$ and $P_T = 6$ GeV. This behavior is due to the large contribution of the Compton term in this range. Such should not be the case in comparing pp and $p\bar{p}$ at large X_T, when pp data from UA6 will become available.

Predictions from Contogouris et al.[24], also shown on figure 15, are in reasonable agreement with the data but indicate a faster rise of the ratio π^-/π^+ with P_T.

Associated particles

1. AFS analysis

At ISR energy one expects, assuming that the Compton diagram is dominant, a jet recoiling against the photon. By measuring the pseudo-rapidity Y_J of this jet (or equivalently its direction) one fixes entirely the kinematics of the subprocess, avoiding any integration on Bjorken x.

In AFS data[25], one requires that $|Y_J| < 0.4$, such that the two x's are almost equal :

$$\frac{d\sigma}{d\,P_T\,dY\,dY_J} = \frac{5\pi\,\alpha\alpha_s(Q^2)}{3}\,\frac{G(x,Q^2)\,F_2(x,Q^2)}{x^2\,s^{3/2}}$$

In this expression $F_2(x,Q^2)$, known from DIS, depends weakly on Q^2 in the relevant region where $x \sim 0.2$. Such is not the case for α_s and $G(x, Q^2)$.

Taking, arbitrarily, $Q^2 = 4/3\ P_T^2$, one can extract $G(x, Q^2)$ as shown in figure 16. The result clearly disagrees with the usual G(x) distribution.

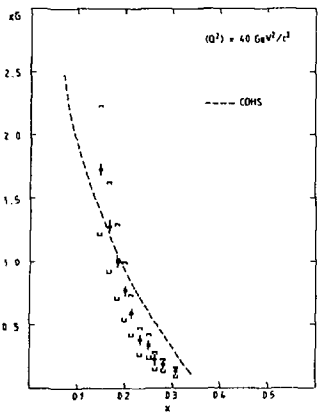

FIGURE 16

xG(x) measurement from AFS analysis using the jet information. The curve, deduced from CDHS data, is similar to DOI.

Aurenche et al.[26] have questioned this procedure and shown that, using the optimized value for Q^2 deduced from the study of inclusive processes, this conclusion is ruled out. As shown in figure 17b, the fast variation of α_s, not properly accounted for in AFS analysis, is responsible for this

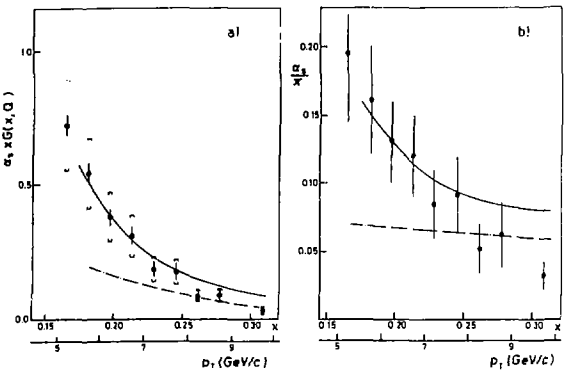

FIGURE 17

Figure (a) is a comparison between $\alpha_s xG(x)$ directly deduced from AFS analysis and a computation[26] (full curve) using the optimised Q^2 definition and DOI. The dashed dotted line uses the definition $Q^2 = 4/3\ P_T^2$. Figure (b) shows the corresponding variation of α_s/π.

behavior. The authors of ref. 26 remark that their procedure is not complete since the optimization should be carried on the γ-jet cross section. Therefore no definite conclusion can be reached about G(x).

It remains that this example illustrates very well the importance of a correct definition of Q^2.

2. WA70

At SPS energy, the jet associated to the direct γ is difficult to define. One may however use the leading particle, charged or neutral, which has a sufficient P_T to be separated from the beam and target fragments. One also assumes, as in the previous example, that the Born diagram is dominant. This procedure is applied by WA70[27], based on an excellent coverage for charged (Ω spectrometer) and neutral particles. It is checked by a Monte Carlo generator using the Born topology plus fragmentation functions given by LUND[28].

For pp data we expect up jets to dominate, coming from the Compton subprocess. This is, to a lesser extent, also true for π^+p. In π^-p, there should be a majority of events with a gluon jet.

One firstly expects a softer fragmentation function for gluons, as indicated experimentally[29]. The predictions are shown in figure 18a from the LUND generator. To define the fraction Z, carried by the leading particle, one uses :

$$Z = P_{T\ HAD}/P_{T\ \gamma}$$

which assumes a perfect balance between the jet and the γ (Born term with no intrinsic K_T effect) to avoid the painful estimate of the jet momentum.

The three reactions give the fragmentation functions shown on figure 18.

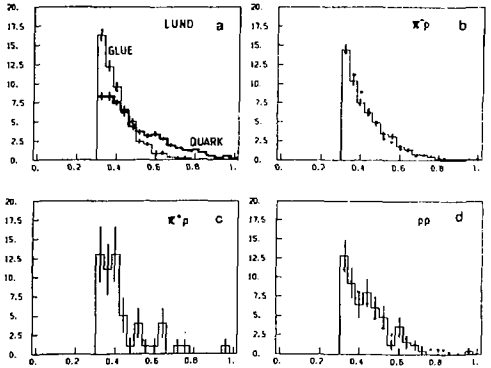

FIGURE 18
Shapes of the fragmentation function for the leading hadron, for quarks (dark line) and gluons (light line) given by the LUND model (a). Experimental distributions from WA70 are adjusted for π^-p (b), π^+p (c) and pp (d) channels.

The fraction of glue versus quark is freely adjusted giving 70 ± 4 % in the case of π^-p and 30 ± 20 % in the case of pp. The statistics on π^+p are too scarce to reach any quantitative conclusion. Let us finally note that if one uses the quark fragmentation function for π^-p, the fit is poor with a χ^2 increasing to 2.5 per degree of freedom.

Secondly, one expects a significant excess of positive charges in pp and π^+p for the leading particles, due to the up quarks, while π^-p should show a much weaker effect. This effect should increase with Z, since very leading hadrons are likely to contain the first generation quark.

Figure 19 shows spectacularly these expected effects. It is also remarkable to notice that the beam fragments, which would be dominantly negative in the

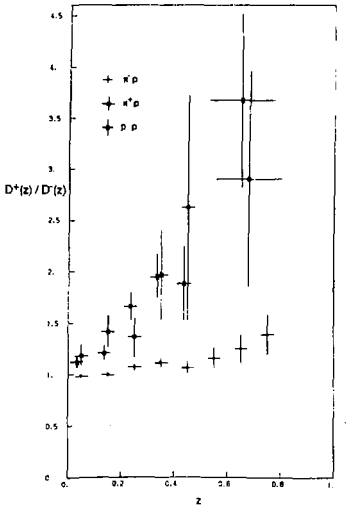

FIGURE 19
The ratio of fragmentation function for positive and negative leading particles measured in WA70 in π^-p, π^+p and pp.

case of π^-p, do not seem to play any significant part since the π^-p data give a positive charge even at low Z.

These very nice data deserve the effort of a more quantitative analysis, using the complete QCD calculations, to confirm the agreement between experiment and the complicated cocktail of diagrams involved in the H.O. calculations.

Summary and conclusions on direct photons

The recent direct photon data which have been presented are well reproduced by perturbative QCD calculations over a large energy domain. A fitting procedure should give precise informations on α_s and G(x). Annihilation dominated processes indicate that $\Lambda_{\overline{MS}}$ = 200 MeV is compatible both with the $\pi^- p$ and the $\bar{p}p$ data. Assuming this value, one can deduce from pp data a gluon structure function slightly softer [$xG(x) \sim (1-x)^{6.5}$], at $x > 0.3$, than DOI.

Associated hadrons confirm, in a semi quantitative way, the underlying mechanisms of direct photon production.

Various improvements can be expected in the near future. Better proton structure function will come from the precise DIS data shown at this conference. Using high statistics $p\bar{p}$ and pp data, which will be available from UA6 with the advent of ACOL, one should measure precisely $\Lambda_{\overline{MS}}$ and G(x).

UA1, with an upgraded calorimeter, should also obtain much better data.

At FNAL, two fixed target experiments are planned, E705 and E706, which will cover the X_T region corresponding to the ISR data.

DRELL-YAN

General picture

At zeroth order, hadroproduction of lepton pairs is described by a quark anti-quark annihilation process (figure 20). If one assumes K_T = 0 for q and $\bar{q}$, the lepton pair has a transverse momentum Q_T = 0. In the lepton pair rest

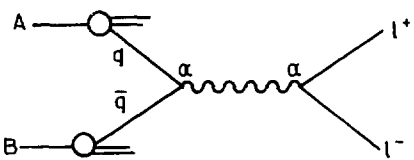

FIGURE 20
Basic subprocess in Drell-Yan.

frame system, in which hadron A and B have the same direction, the polar angle of the lepton with respect to this direction follows a $1 + \cos^2\theta$ distribution.

Knowing the stucture function from B (a proton for instance), one can extract the structure function from A. As well known, this has been the unique method to measure the mesonic structure functions. One can as well measure the proton sea quark structure functions in the pp process, also accessible from DIS experiments.

There are large corrections to this zero order behavior which are well explained by perturbative QCD. The cross section is multiplied by a K factor of about 2 which has been calculated at order α_s. In spite of this very large correction, the validity of the perturbative approach is maintained by summing at all orders the largest part of this correction (exponentiation of the "soft gluon" terms). At the moment the full $O(\alpha_s^2)$ calculations are not available.

Q_T distributions can also be computed using soft gluon summation methods. This technique, used by Altarelli et al.[30], successfully describes the W and Z transverse momentum distributions. As another example, the ISR data from R110[31], which has recently completed its analysis, are shown in figure 21. To illustrate the validity of this description in a large energy domain, one can plot $\langle Q_T \rangle$, the average of the distribution, versus $\sqrt{s}$. QCD predicts that :

$$\langle Q_T^2 \rangle = \alpha_s(Q^2)\ s\ F(\tau, \ell n\ Q^2) + C \qquad \text{with} \quad \tau = M^2_{\ell^+\ell^-}/s$$

Provided τ remains constant and given the small variations due to Q^2, QCD predicts a linear variation with s.

Figure 22 shows that this description works quite well[32].

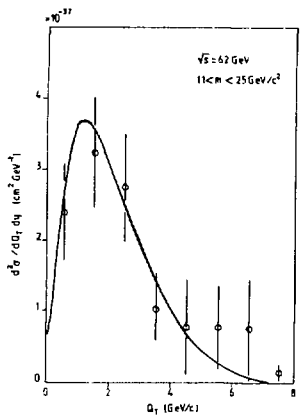

FIGURE 21
$pp \to e^+e^-X$ Q_T distribution measured by R110 at $\sqrt{s}$ = 62 GeV for masses between 11 and 25 GeV. The curve is from ref.30.

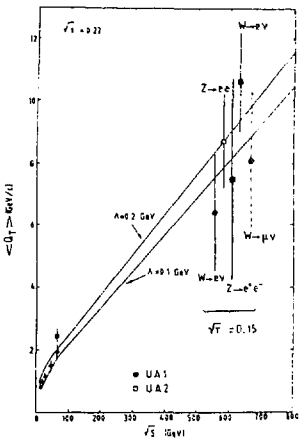

FIGURE 22
Energy dependence of the average transverse momentum in Drell-Yan processes from ISR data (low energy points) and UA1 and UA2 measured from W and Z data. QCD predictions are for Λ = 200 MeV (upper curve) and Λ = 100 MeV (lower curve).

How accurately do we know K ?

High statistics Drell-Yan experiments like NA10 for $\pi^- W \to \mu^+\mu^-$ or E605[34] for $pCu \to \mu^+\mu^-$, provide very precise data which are challenging at an unprecedented level QCD predictions. NA10 data[35] are remarkably well reproduced up to $\tau^{1/2} \sim 0.4$ by QCD calculations. In a recent paper, Aurenche and Chiappetta[36] have included the optimization technique discussed for direct photon (Q^2 definition is also ambiguous in D.Y.) in the usual calculation. From figure 23 one would conclude that precise Drell-Yan data can provide a valid measurement of $\Lambda_{\overline{MS}}$. For higher values of $\tau^{1/2}$ (figure 24), however, there is a significant is a significant disagreement with the data, which casts serious doubts on the whole procedure. A possible way out, discussed in next §, is to incriminate nuclear effects.

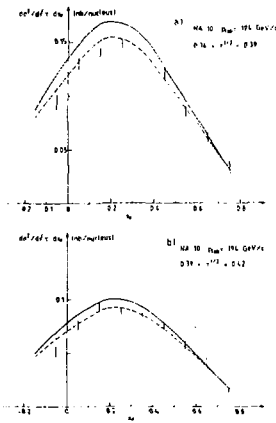

FIGURE 23
Differential Drell-Yan cross section measured in NA10[35] in two τ regions. Data have been corrected for Fermi motion. Predictions[36] are for $\Lambda_{\overline{MS}} = 200$ MeV(full curve) and $\Lambda_{\overline{MS}} = 100$ MeV(dashed curve).

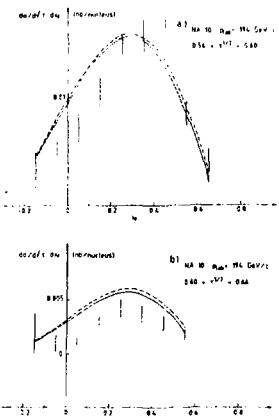

FIGURE 24
Same as figure 23 for higher τ values.

Nuclear effects

1. K Factor

Nuclear effects are directly observed in NA10 by comparing data at 194 GeV and 286 GeV taken simultaneously on tungsten and deuterium[37]. Recently Chiappetta and Pirner[38] have included nuclear effects in the Drell-Yan calculation using two approaches which are consistent with the DIS data. The results are shown in figure 25 together with the NA10 data. At large τ and low x_F,

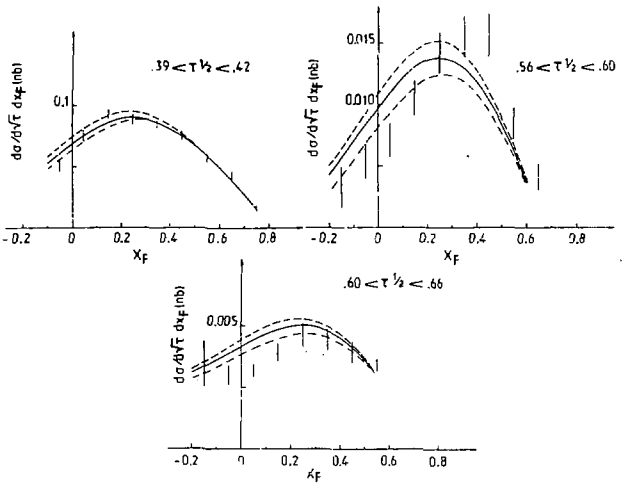

FIGURE 25
Predictions for Drell-Yan cross sections with no EMC effect (dashed), Q^2 rescaling model (full curve) and x rescaling model (dashed dotted), from ref. 38. The dotted curve corresponds to the zero order prediction. Data are from NA10 experiment .

which corresponds to the large Bjorken x part of the target structure function, the nuclear effect is well observed. The agreement with the data is significantly improved although not perfect. Data[39] at 286 GeV confirm the same trend.

At this stage, it seems fair to conclude that nuclear effects are not well controlled enough to allow a very precise test of QCD through the Drell-Yan mechanism.

2. Q_T distribution

Taking the ratio of deuterium and tungsten data, NA10[40] obtains the curves given in figure 26. Nuclear effects induce a large increase of the cross section at large Q_T. This effect is less marked at high energy. Since the

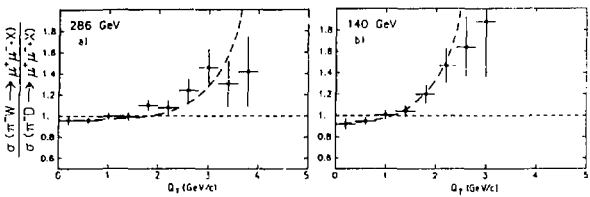

FIGURE 26
Ratio of cross sections measured on tungsten and on deuterium in NA10 versus transverse momentum. Figure (a) is at 286 GeV, (b) at 140 GeV. Curves are from ref. 38.

integrated cross section shows no shadowing effect, the enhancement at large Q_T is compensated at small Q_T as indicated by the data below 1 GeV. In ref. 38, this behavior is attributed to a multiple scattering effect of the incoming parton inside the nucleus. Parametrizing the quark-nuclear cross section σ_{qN} as a function of the virtuality Q^2 of the quark, the authors of ref. 38 can reproduce the data of NA10 (curves in figure 26). In the present case, the effect is beneficial since it helps us in understanding the virtual quark cross section on a nucleus.

Angular distribution

When Q_T differs from 0, the definition given in the introduction is not unique since $\vec{P}_A$ and $\vec{P}_B$ are not collinear. Collins and Soper[41] (C.S.) have proposed to take the external bisector of these two directions.

This choice will balance, on average, the effect of intrinsic K_T contributions from parton A and parton B. The angular distribution of the lepton follows the general form[42] :

$$\frac{d\sigma}{d\cos\theta\, d\phi} \propto 1 + \lambda \cos^2\theta + \mu \sin 2\theta \cos\phi + \frac{\nu}{2} \sin^2\theta \cos 2\phi$$

$\mu = 0$ from perturbative QCD. This result is not altered by intrinsic K_T effects in the C.S. frame provided that, on average, K_T from the target and from the projectile are equal.

In perturbative QCD, λ deviates from 1, while ν is correlated to λ though a Callan-Gross type relation : $\lambda = 1 - 2\nu$.

In a paper submitted to this conference, the NA10 collaboration presents a new analysis of their data[43]. While the previous paper[44] was only taking into account the hard component of QCD valid at large Q_T, the present interpretation considers the soft gluon contribution terms which are dominant in the Q_T domain covered by NA10. This is shown in figure 27 from ref. 45 where, although not

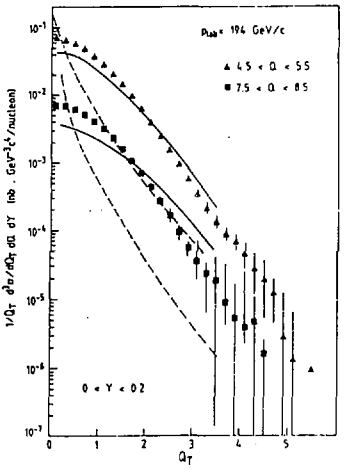

FIGURE 27
Distribution of transverse momenta for two mass regions measured in NA10. Full curves are deduced from ref. 30. Dashed curves take into account the first order calculation with no soft gluon summation.

perfect, the theoretical predictions based on soft gluon summation techniques give the right order of magnitude for the Q_T distribution. In the same figure, one can observe that the hard component term is too low by an order of magnitude.

Figure 28 shows the NA10 data at three energies. The prediction from ref.45 agree reasonably well for λ and μ, while there are significant deviations

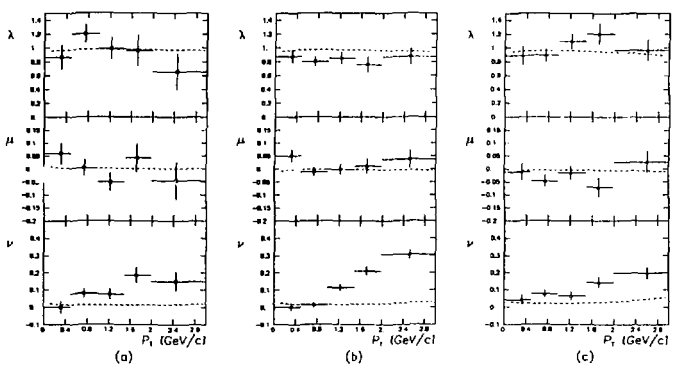

FIGURE 28

λ,μ and ν (defined in the text) versus Q_T at three energies using NA10 data. The C.S. frame is used. The large Bjorken x region (> 0.7) is excluded for the projectile. The dashed curves are from ref. 45.

observed for ν at large Q_T. This disagreement cannot be blamed on higher twist effect[46] since the high Bjorken x region for the projectile has been excluded from these data. The Callan-Gross type relation previously mentioned is evidently broken.

This would suggest a non perturbative origin for the effect. In this prospect, it seems however surprising to observe an increase of the deviation with Q_T.

Summary and conclusions on Drell-Yan

The bulk of Drell-Yan data is well reproduced by perturbative QCD. High statistics data from NA10 show, however, significant deviations which can be partly attributed to nuclear effects. In this respect one may conclude that high accuracy tests of QCD are difficult with nuclear targets. One may alternatively point out that Drell-Yan, a well understood mechanism, can be used as a probe to understand quark-nuclear mechanisms.

The angular decay distributions at SPS energy are not well understood. Theory would be in trouble if this behavior persists at high energy. For instance, one may hope to gather a sufficiently large lot of W/Z in the near future to check for such deviations.

LOW P_T ELECTRONS

The ratio e/π, measured at ISR, is not understood at low P_T from classical sources. This well known puzzle is illustrated by figure 29 where the various results obtained at ISR are represented. At low P_T, the dominant source of leptons comes from virtual bremsstrahlung originating from the final hadrons. It is of course legitimate to consider, at a previous stage, the "parton soup" which boils down into these hadrons. This picture was proposed a long time ago by Bjorken and Weisberg[47] who suggested that lepton pairs are simply produced by annihilating quarks and antiquarks present in this soup.

As pointed by a group from Bratislava[48], such mechanism should show a very specific correlation with the final state multiplicity m. While Drell-Yan process is independent of m and bremsstrahlung increases linearly with m,

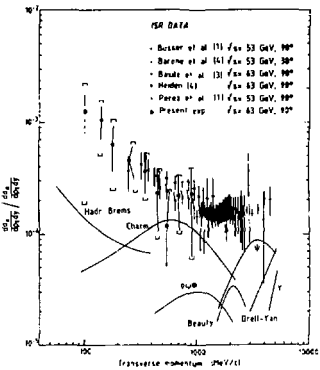

FIGURE 29
Summary on e/π measurements from ISR. The classical contributions are shown through the various curves. AFS data (•) extend down to very low P_T.

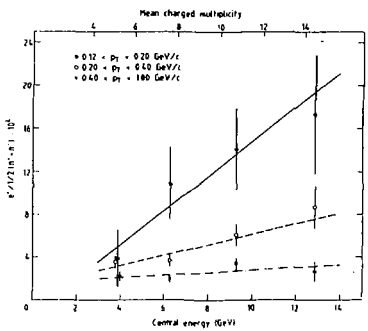

FIGURE 30
Ratio e^+/π measured in AFS versus charged multiplicity or, equivalently, versus central energy as measured from the calorimeter. Three transverse momentum bands are considered. Straight lines are adjusted to the data.

parton annihilations vary like the product of quark and antiquark density and thus increase quadratically with m :

$$P_{annihilation} \sim \frac{dN}{dY}(q)\,\frac{dN}{dY}(\bar{q}) \sim \left(\frac{dN_\pi}{dY}\right)^2$$

$$\text{Since } \frac{dN}{dY}(q) \sim \frac{dN_\pi}{dq}$$

AFS[49] measures the rate of direct positrons (electrons are avoided since they can originate from Compton scattering on atomic electrons) in correlation with dN/dY, the hadron density or, equivalently, with E_T the transverse energy measured in the central calorimeter. They use a powerful electron identification, combining Cerenkov, time of flight, dE/dX and electromagnetic calorimetry (NaI). They reject and control very efficiently the conversion and Dalitz pair background by using, in particular, a low field configuration which allows a pair reconstruction down to 2 MeV.

The correlation is shown on figure 30 where one observes a linear increase of e/π with respect to the mean charged multiplicity (or to E_T) as expected in the Bjorken mechanism. A flat distribution, expected in the bremsstrahlung case, would give a confidence level of 0.7 %.

Are these positrons produced in pairs, as one would expect in the quark antiquark mechanism ? Hadroproduction of pairs at low mass has been studied at low energy by various experiments. These results were also not quantitatively understood from classical sources. AFS has extended[50] these study reaching masses below 100 MeV. Figure 31 summarizes the presently available data. The cross section derived by AFS depends strongly on acceptance corrections which, in turn, depend on the momentum distributions assumed in the Monte Carlo generation. With this caveat, one can compare AFS data to a calculation of the Bratislava group (dashed curve in figure 31) to a mere $1/M^2$ extrapolation given by the low energy results.

The multiplicity correlation is also clearly observed as shown on figure 32. Since the rate of measured pairs at low masses is sufficient to saturate e/π at low P_T, one may conclude that a consistent picture for this phenomenon is finally emerging from AFS measurements.

One cannot however turn this into a success of theory, since the quark-antiquark annihilation process under consideration is working in a kinematical region carefully avoided by all perturbative QCD experts !

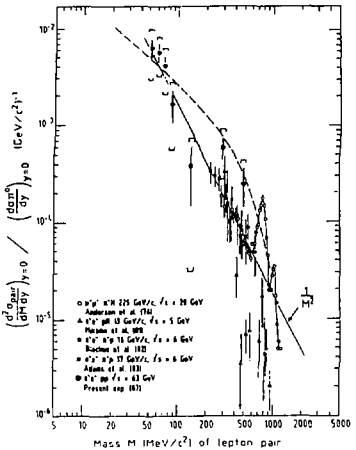

FIGURE 31
Summary on lepton pair results (normalised on π^0 data). AFS experiment results (•) extend to very low masses. The dashed curve is from ref. 48. The full curve is a $1/M^2$ adjustement to the data.

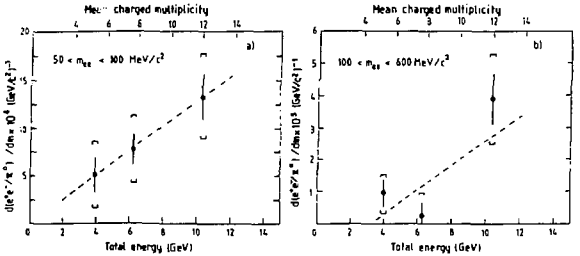

FIGURE 32
Mean multiplicity dependence of the pair production cross section measured by AFS for two mass bands. Straight lines are adjusted to the data.

AFS has also measured the rate of real γ as described in ref. 51 submitted to this conference. They observe a rather weak signal but which appears consistent with the low energy results. Let me recall that Chliapnikov et al.[52], at $\sqrt{s}$ = 12 GeV, had observed in $K^+p \to \gamma$, at P_T below 100 MeV, a large γ signal in excess of the standard bremsstrahlung expectations.

AFS and low energy data are shown on figure 33. Let me now explain further this complicated plot. On general grounds[50], virtual bremsstrahlung should be

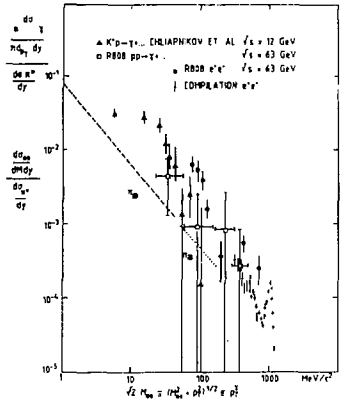

FIGURE 33
Direct photon data and low mass pair results from AFS are compared as explained in the text.

α times real bremsstrahlung. The authors of ref. 50 have tried accordingly to compare both sets of results. Kinematically, a small "bricolage" is necessary to relate P_{T_γ} to the mass and transverse momentum of the pairs. This is done through the usual concept of transverse mass, i.e. $m_T = \sqrt{m^2 + P_T^2}$. As a result, we see on figure 33 that direct γ data compare reasonably well to pair data and are sitting largely above the bremsstrahlung curve (dotted and dashed curves).

Summary and conclusions on low P_T electrons

AFS results are providing a very interesting clue to understand the e/π puzzle. It seems, from the phenomenological point of view, that the data can be reproduced via final state partons electromagnetic interactions. These processes, as already mentioned, are very soft and one is clearly leaving the safe domain where the concepts of perturbative QCD, discussed so far, are valid.

As rightly stressed in ref. 49, a clear understanding of the phenomenon is necessary in view of the quark-gluon plasma studies, where one expects real and virtual photons to provide the most readable information.

CONCLUSIONS

For each of the three themes discussed in this report, I have given my conclusions. At this point, I can only stress once more that recent and near future data on direct photons should allow a precise determination of α_s and G(x). One may also note that photoproduction at large transverse momentum, not covered here since no new data were presented at this conference, is providing very healthy information on the same processes and that the field should develop with the advent of HERA.

For what concerns Drell-Yan, future prospects appear also very good with the large samples of W/Z expected from $p\bar{p}$ collider data. A very precise test of QCD seems possible at SPS but would require high statistics on deuterium to avoid the uncertainties coming from nuclear effects.

ACKNOWLEDGEMENTS

I would like to thank the Conference organizers, particularly Prof. Paul Söding, for the pleasant atmosphere and excellent organisation of this Symposium. The help of Dr. W. Zeuner in preparing this talk is also appreciated.

I would also like to thank M. Albrow, P. Aurenche, R. Baier, P. Chiappetta, T. Cox, M. Denegri, L. DiLella, M. Fontannaz, M. Martin, B. Mours, D. Schiff, M. Werlen, W. J. Willis among many others for enlightening discussions on the topics under review.

I finally thank Mrs O. Clavelo and Mrs M. Debest for their efficiency and patience in preparing this paper.

REFERENCES

1) Recent reviews :

J.P. Rutherfoord, Proc. of the 1985 Int. Symp. on Lepton and Photon Interactions, Kyoto, 662 (1986)
D. Treille, Proc. of the Int. Europhysics Conf. on HEP, Bari, 793 (1985)

See also, on direct photons :
T. Ferbel and W.R. Molzon, Rev. Mod. Phys. 56, 181 (1984)

Direct photons

2) R806 Collaboration, E. Anassontzis et al, Z. Phys. C13, 277 (1982)

3) R110 Collaboration, A.L.S. Angelis et al, paper in preparation

4) UA1 Collaboration, B. Mours, private communication

5) UA2 Collaboration, J.A. Appel et al, Phys. Lett. B176, 239(1986)

6) P. Aurenche et al, Phys. Lett. 140B, 87 (1984)

7) A.P. Contogouris and H. Tanaka, Phys. Rev. D33, 1265(1986)

8) J.F. Owens, Rev. of Mod. Phys. 59, 465(1987)

9) P. Aurenche et al, Prompt photon production at large P_T. Scheme invariant QCD predictions and comparison with experiment. Contributed paper 201 to this conference and LPTHE Orsay 87/30

See also : P. Aurenche et al in Nucl. Phys. B286, 509(1987)

10) P.M. Stevenson, Phys. Rev. D23, 2916(1981)

11) H.D. Politzer, Nucl. Phys. B194, 493(1982)

12) G. Grunberg, Phys. Lett. 95B, 70(1980)

13) E.L. Berger, Phys. Rev. D26, 105(1982)

14) E.L. Berger et al, Nucl. Phys. B239, 52(1984)

15) T. Akesson et al, Phys. Lett. 118B, 178(1982)

16) D.W. Duke and J.F. Owens, Phys. Rev. D30, 49(1984)

17) J.F. Owens, Phys. Rev. D30, 943(1984)

18) G.A. Voss, rapporteur's talk at this conference

19) UA6 Collaboration, A. Bernasconi et al, preprint CERN-EP/87-120 (1987)

20) NA24 Collaboration, C. De Marzo et al, Phys. Rev. D36, 16 (1987)

21) WA70 Collaboration, M. Bonesini et al, High transverse momentum prompt photon production by π^- and π^+ on proton at 280 GeV/c, contributed paper 172 to this conference

22) WA70 Collaboration, M. Bonesini et al, Production of high transverse momentum prompt photons and neutral pions in proton-proton interactions at 280 GeV/c, contributed paper 171 to this conference

23) P. Aurenche et al, to appear in Nucl. Phys. B and ref. 9

24) A.P. Contogouris et al, Phys. Rev. D32, 1135(1985)

25) AFS Collaboration, T. Akesson et al, Z. Phys. C34, 293(1987)

26) P. Aurenche et al, Phys. Lett. 169B, 441(1986)

27) WA70 Collaboration, M. Bonesini et al, A study of the structure of events triggered by direct photons in $\pi^- p$, $\pi^+ p$ and pp collisions at 280 GeV/c, contributed paper 166 to this conference

28) H.O. Bengtsson et al, Comp. Phys. Comm. 34, 251(1985)

29) W. Hofmann, rapporteur's talk at this conference.

Drell-Yan

30) G. Altarelli et al, Phys. Lett. 151B, 457(1985)

31) R110 Collaboration, A.L.S. Angelis et al, Phys. Lett. 147B, 472(1984). The result presented here contains the whole statistics

32) C. Stubenrauch, thesis, Université Paris-Sud (June 1987). Preprint CEA-N-2532 (Saclay).

33) UA2 Collaboration, R. Ansari et al, Phys. Lett. 194B, 158(1987)

34) E605 experiment. See, for instance, J.A. Crittenden et al, Phys. Rev. D34, 2584(1986)

35) NA10 Collaboration, B. Betev. et al, Z. Phys. C 29, 439(1985)

36) P. Aurenche and P. Chiappetta, Z. Phys. C 34, 201(1987)

37) NA10 Collaboration, P. Bardalo et al, Phys. Lett. 193B, 368(1987)

38) P. Chiappetta and H.J. Pirner, Nucl. Phys. B291, 765(1987)

39) L. Kluberg, private communication.

40) NA10 collaboration, P. Bordalo et al, Phys. Lett. 193B, 373(1987)

41) J.C. Collins and D.E. Soper, Phys. Rev. D16, 2219(1977)

42) C.S. Lam and W.K. Tung, Phys. Rev. D18, 2447(1978)

43) NA10 Collaboration, M. Guanziroli et al, Angular distributions of muon pairs produced by negative pions on tungsten, contributed paper 270 to this conference

44) S. Falciano et al, Z. Phys. C31, 513(1986)

45) P. Chiappetta and M. Le Bellac, Z. Phys. C32, 521(1986)

46) E.L. Berger and S.J. Brodsky, Phys. Rev. Lett. 42, 940(1979)

Low P_T electrons

47) J.D. Bjorken and H. Weisberg, Phys. Rev. D13, 1405(1976)

48) V. Cerny et al, Z. Phys. C31, 163(1986)

49) AFS Collaboration, T. Akesson et al. The production of prompt positrons at low transverse momentum increases with the square associated charged multiplicity, contributed paper 118 to this conference and preprint CERN-EP 187-16

50) AFS Collaboration, T. Akesson et al. Production of low-mass electron-positron pairs in proton-proton collisions at a center-of-mass energy of 63 GeV, contributed paper 117 at this conference.

51) AFS Collaboration, T. Akesson et al. Search for direct γ production at low transverse momentum in 63 GeV pp collisions, Contributed paper 119 to this conference and preprint CERN-EP/87-85

52) P.V. Chliapnikov et al, Phys. Lett. 141B, 276(1984)

DISCUSSION

J. Thompson, University Pittsburgh

Will there be further improvement at high X_T in the direct γ production from NA24 and WA70 before the data from FNAL are available ?

F. Richard, L.A.L., Orsay

NA24 has stopped taking data, WA70 is still running and will increase significantly its statistics on $\pi^- p$. You should however remember that systematic errors are already limiting these data.

M.N. Kienzle, Geneva University

WA70 data from 1986 (not included in the present analysis) will improve the high P_T $\pi^- p \to \gamma X$ statistics by a factor ~3. The systematic errors may also go down to 15-20%, with further analysis.